REEXAMINATION OF GLOBAL CARBONATE ABUNDANCES USING TES DATA. T. D. Glotch[1] and A. D. Rogers[1], [1]Department of Geosciences, Stony Brook University, Stony Brook, NY. tglotch@notes.cc.sunysb.edu

Introduction: The recent discovery of carbonate-rich outcrops in the Nili Fossae region of Mars using data returned by the Compact Reconnaissance Imaging Spectrometer for Mars (CRISM) instrument [1] as well as indications of 2-3% carbonate in alkaline soils at the Phoenix landing site [2] have brought into question the hypothesis that much of martian history has been dominated by an acidic weathering regime. Carbonate minerals were previously detected by the Thermal Emission Spectrometer (TES) at the 2-5% level in the globally homogenous martian fines [3]. This detection was confirmed by the Spirit Mini-TES instrument [4]. Until the recent CRISM detection, however, carbonates had not been detected in outcrop form on Mars, leading to several hypotheses regarding their absence [5-6].

A focus of recent studies has been the possibility of carbonate breakdown by incident UV radiation. In this scenario, carbonate minerals would be dissociated, releasing CO_2 into the atmosphere and leaving behind oxide or, perhaps hydroxide remnants. Laboratory studies of carbonate breakdown under martian conditions have yielded conflicting results [7-8].

Previous global mapping of carbonate mineralogy using TES data [9] utilized only two mineral end-members: calcite ($CaCO_3$) and dolomite ($(Ca,Mg)CO_3$). In this study, we searched the TES data set for evidence of carbonate, hydrous carbonate, and carbonate decomposition products at 8 ppd using an expanded mineral library including siderite ($FeCO_3$), magnesite ($MgCO_3$), lime (CaO), portlandite ($Ca(OH)_2$), periclase (MgO), brucite ($Mg(OH)_2$), hydromagnesite ($Mg_5(CO_3)_4(OH)_2 \cdot 4H_2O$, dypingite ($Mg_5(CO_3)_4(OH)_2 \cdot 5(H_2O)$, monohydrocalcite ($CaCO_3 \cdot H_2O$), and nesquehonite $Mg(HCO_3)(OH) \cdot 4H_2O$.

Methods: *Sample selection and preparation.* Siderite and magnesite samples were acquired from Wards Natural Science, and hydromagnesite, nesquehonite, and dypingite samples were acquired from Excalibur Mineral Corporation. A sample of monohydrocalcite was loaned to us by R. J. Reeder. Reagent-grade powders of portlandite, periclase, and brucite were acquired from Fisher Scientific. Lime was produced by heating reagent-grade calcite overnight at 875 °C. All samples were powdered and pressed into compact pellets for specular reflectance measurements.

Specular reflectance measurements were carried out on a Nicolet 6700 FTIR spectrometer fitted with an FT-30 specular reflectance accessory at Stony Brook University. Mid-IR spectra (400-4000 cm^{-1}) were acquired using a DLaTGS detector with a KBr window and a KBr beamsplitter. Far-IR spectra (100-600 cm^{-1}) were acquired using a DLaTGS detector with a polyethylene window and a Nicolet Solid Substrate beamsplitter.

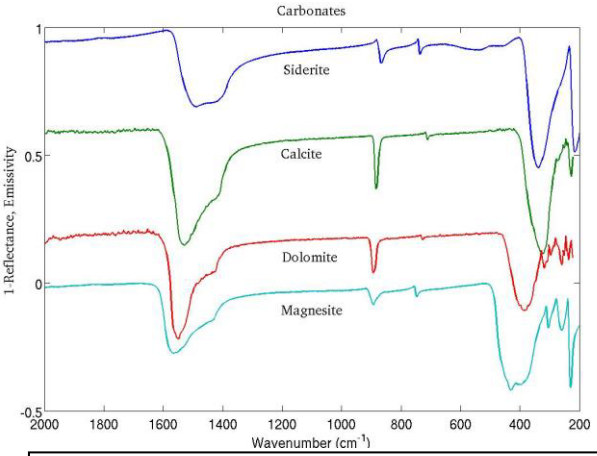

Figure 1. Carbonate spectra used in this study. Calcite and dolomite spectra are from the ASU TES emissivity library. Siderite and magnesite spectra were collected in reflectance at SBU and converted to emissivity.

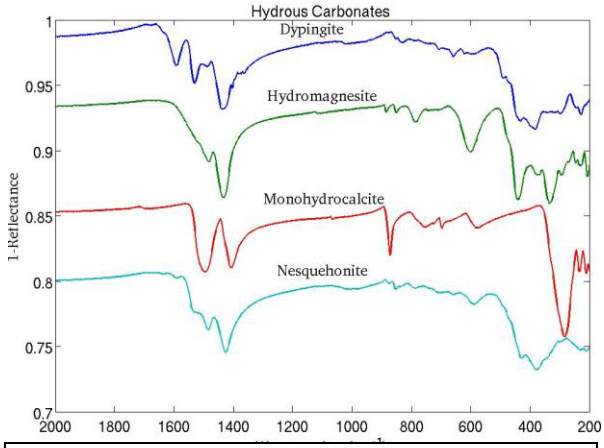

Figure 2. Hydrous carbonate spectra used in this study. All spectra were acquired in specular reflectance mode at SBU and converted to emissivity.

TES data mapping. Spectra were converted to emissivity via Kirchhoff's Law (ε=1-R) and added to a mineral spectral library based on [10]. The number of library spectra from [10] was reduced slightly to make room for the additional spectra acquired for this study. High quality TES data were binned to 8 ppd (excluding surfaces with albedos >0.16). The binned emissivity spectra were deconvolved using four distinct libraries. The first deconvolution utilized the full spectral li-

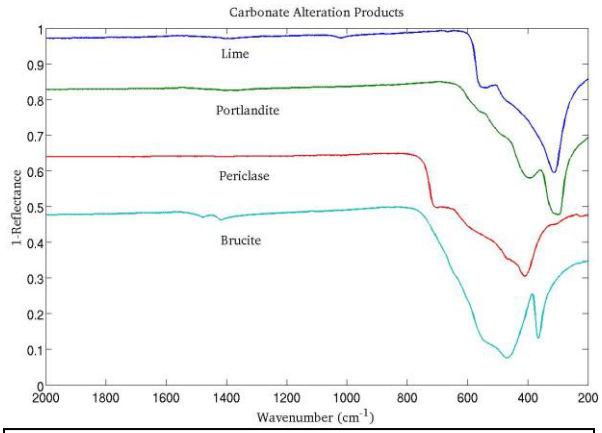

Figure 3. Carbonate decomposition product spectra used in this study. All spectra were acquired in specular reflectance mode at SBU and converted to emissivity.

brary. The other three deconvolution models utilized libraries containing the endmembers from [10] in addition to one of the following: (1) only the anhydrous carbonates, (2) only the hydrous carbonates, or (3), only the carbonate decomposition products.

Results: Results from the mineral mapping are shown in Figure 4, where the abundances of carbonates, hydrous carbonates, and carbonate alteration products are shown as red, green, and blue, respectively. Abundances were determined from the limited libraries discussed above. As can be seen in Figure 4, hydrous carbonates are the dominant modeled phases. The uniformly high modeled abundance of hydrous carbonates are highly suspect and are not consistent with NIR observations. A comparison with results from all four libraries indicates that hydrous carbonates are substituting for clinopyroxene in the deconvolution model, but the reasons for this are unclear. It will be difficult to confirm the presence of these minerals using TIR data. Anhydrous carbonates do not appear to be present in geographically contiguous regions with one or two exceptions, supporting previous work of [1,3,9]. One or two pixels appear to show carbonate enrichment in the Nili Fossae region, consistent with the recent CRISM detection [1]. A small region of high carbonate concentration on the northeast rim of Hellas Basin will be investigated further using TES, THEMIS, and CRISM data. Finally, carbonate decomposition products appear at high concentrations in a few geographically distinct regions, including Syrtis Major and a few areas in the southern highlands. Future work will involve careful analysis at higher spatial resolution to determine if the presence or absence of one or more of these phases can be confirmed.

Conclusions: This work generally supports previous results that carbonates are not present in large outcrops on the martian surface. Indications of several local-scale outcrops of carbonates and carbonate decomposition products will be investigated in more detail in future work.

References: [1] Ehlmann B. L. et al. (2008) *Science, 322,* 1828-1832. [2] Boynton W. V. et al. (2008) *EOS Trans. AGU 89(53)*, Abstract U14A-03. [3] Bandfield J. L. et al. (2003) *Science, 302*, 1084-1087. [4] Christensen P. R. et al. (2004) *Science, 305*, 837-842. [5] Bullock M. A. and J. M. Moore (2007) *GRL, 34*, L19201. [6] Halevy I. et al. (2008) *Science, 318*, 1903-1907. [7] Mukhin L. M. et al. (1996) *Nature, 379*, 141-143. [8] Quinn R. et al. (2006) *Astrobiology, 6*, 581-591. [9] Bandfield J. L. (2002) *JGR, 107*, 5042. [10] Rogers, A. D. et al. *(2009) Icarus*, in press.

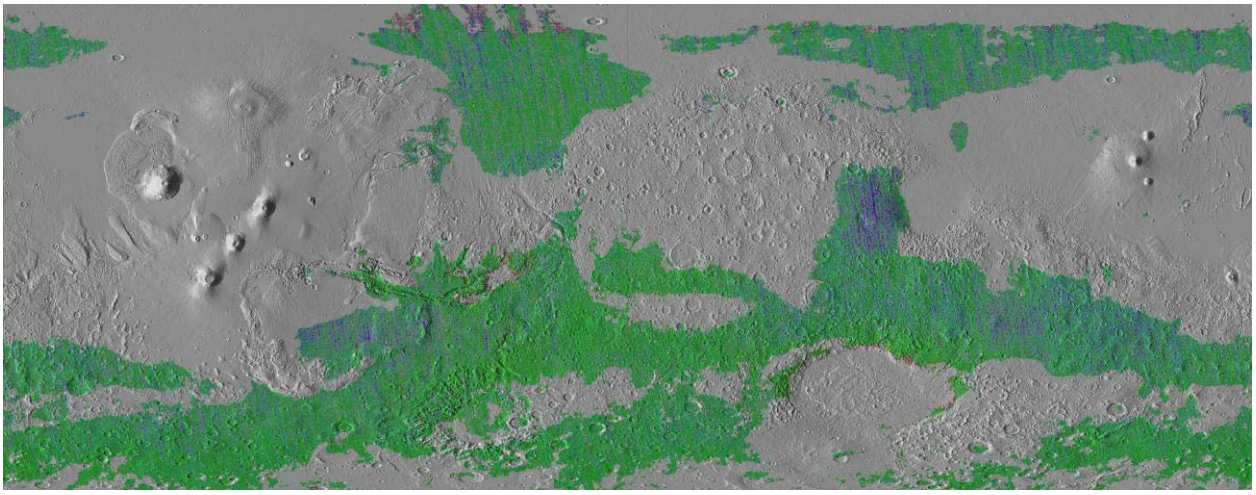

Figure 4. Global distribution of carbonates (red), hydrous carbonates (green), and carbonate decomposition products (blue) based on deconvolution of binned TES emissivity data. The RGB color stretch is from 0 to 0.3 concentration in each color channel. Areas with albedos higher than 0.16 are masked out and were not included in this study.